Transport from Extended Surfaces

STANLEY K. STYNES and JOHN E. MYERS

Purdue University, Lafayette, Indiana

It is common practice among manufacturers and users of heat transfer equipment to specify extended surface, heat exchangers where a high heat flux per unit length of heat transfer element is desired. As a result considerable attention has been given in the literature to the various kinds of extended surface which might provide these high fluxes. Jakob (*1*) and others (*2, 3*) have developed solutions to the differential equations defining the temperature distribution within the material of the extended surfaces. In general they have assumed that the local transport coefficient is uniform over the surface. Knudsen and Katz (*4*) have presented experimental results for mean transport coefficients for flow in an annular space past rectangular fins external to the inner tube. Their work is typical of the experimental studies available in the literature (*5, 6, 7*).

More recently Tani et al. (*8*), Roshko (*9*), and Savage and Myers (*10*) have presented results of local pressure measurements in fin spaces which would indicate that the local transport coefficients might vary significantly over the surface of a fin. This conclusion is substantiated by the results of Harris and Wilson (*11*) who measured local heat transfer coefficients for a single finned surface in a wind tunnel. The purpose of the present work is to investigate the nature of transport from extended surfaces with the intent of defining the local character of the flow and the transport mechanism as it is affected by variations in geometrical parameters.

On the assumption that conditions are such that mechanisms for transport of mass and heat are similar (*12*), the same relative variation of local coefficient should be obtained regardless of which quantity is chosen for transport. The dissolution of solid surfaces to determine the nature of local transport has been used frequently in the past (*13, 14, 15, 16*) for a variety of shapes. The rate of dissolution of the solute must be low enough to justify the assumption that the velocity normal to the dissolving surface is negligible. This condition is necessary to achieve similarity between mass and heat transport for similar surfaces.

It is much easier to measure the local rate of dissolution of the soluble surface of a flat fin, with standard micrometer instruments, than to attempt to provide a fin with sufficient thermocouples for local temperature measurements and still maintain a homogeneous path for the flow of heat to its surface. Consequently it was decided to measure the rate of dissolution of benzoic acid by water from the surface of fins for various combinations of fin spacing, fin height, free-channel width, and Reynolds number.

The rate of transport from a fin to the bulk of the fluid in the main stream is controlled by two coupled mechanisms: the local resistance to transport from the finned surface, that is molecular and eddy diffusion through the boundary layer at the fin surface; and the rate of mixing between the fluid in the fin space and that in the main stream. A measure of the significance of the second effect is the mean residence time of the fluid in the fin space, that is the average time a given element of fluid remains within the fin space before returning to the main stream. A comparison of the variation of mean residence times and local transport coefficient with changes in the experimental parameters should provide a basis for determining whether one of the two mechanisms controls the rate of transport from the fin to the main stream.

S. K. Stynes is at Wayne State University, Detroit, Michigan. J. E. Myers is currently on sabbatical leave as Fulbright lecturer at the University of Toulouse, France.

LOCAL COEFFICIENTS

Experimental

One common form of extended surface consists of transverse square fins either external or internal to a tube with flow parallel to the axis of the tube, that is perpendicular to the fin surface (Figure 1). This design was simulated in a way which would be convenient for visual studies as well as for measuring local transport coefficients. Thus the experimental work consisted of measurements of rates of dissolution for open channel flow past soluble transverse fins cast from benzoic acid. A water table was built specifically for this purpose.

The water supply for the channel passed from a calming reservoir through six 16-mesh wire screens and then between converging walls into the main channel. With no fins present in the channel potassium permanganate crystals gave streak lines essentially parallel to the channel walls. The volumetric rate of flow was controlled by a valve in the feed line to the reservior and metered by a rotameter in the same line. The liquid level in the channel was maintained by an adjustable sluice gate at the end of the channel which was capable of holding any desired level within 1/32 in. The water feed was deaerated, tap water pumped from a 500-gal. storage tank. After passing through the channel the water was discharged to a drain. The 500-gal. capacity allowed about 1½ hr. running time at the maximum rate used in the experiments. The table was isolated from the rest of the room by ⅝-in. soft rubber gaskets which minimized vibration caused by surrounding equipment. The underside of the plate glass table top was covered with graph paper containing 20 sq./in. A fluorescent light fixture lit up the entire channel from underneath.

The test section consisted of a brass slab 30-in. long and ¾ in. thick slotted to hold brass fins. This slab (1½ in. deep) was clamped to one wall of the channel. The liquid level was maintained 1-1/16 in. deep, and the brass fins were 1¼ in. deep. For the dissolution studies approximately 1/16 in. of metal was removed from each of two of the fins. This space was filled with benzoic acid. Measurement of the thickness of

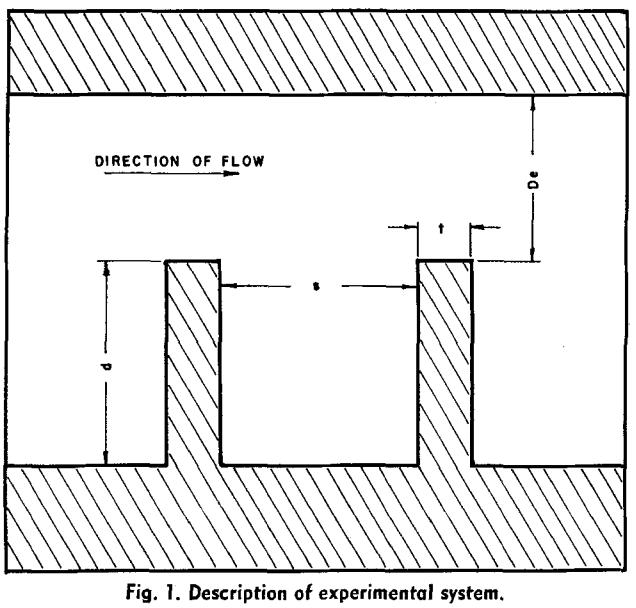

Fig. 1. Description of experimental system.

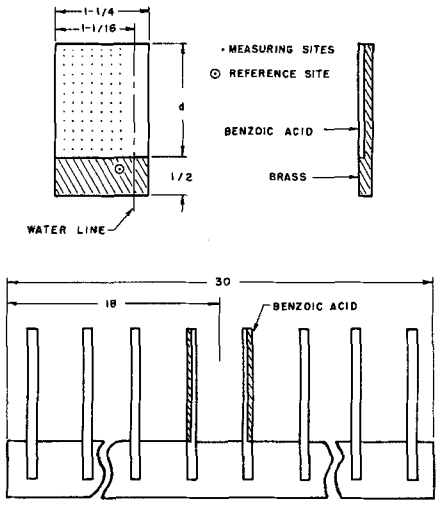

Fig. 2. Benzoic acid fin and fin holder.

the benzoic acid layer before and after each run was made with a dial indicating micrometer gauge which was calibrated in increments of 0.00005 in. (and could be read to 0.00002 in.). A special jig was made which held the fin during measuring and made it possible to locate a given grid point anywhere upon the fin surface within 1/128 of an inch.

Benzoic acid was chosen as the solute to be used in this study. It could be cast in place and adhered firmly to the brass surface. It machined easily giving a smooth finished surface. Operating with water at 25°C. gave measurable but small dissolution rates over a 1-hr. run. The maximum change in thickness of the benzoic acid was found to be less than 0.03 in./hr., and the average change was about 0.005 in./hr. Surface measurements could be made with an error of less than 2% based upon the average dissolution rate of 0.005 in.

Surface measurements were made relative to a selected reference point on the brass portion of the fin, see Figure 2. Measurements were made before and after each run in order to determine the change in thickness of the benzoic acid layer. Each point on Figure 3 represents a measurement made upon the surface of a typical 1¼ in. high fin. Several measurements were made along the tip of the fin, seven more 1/16 in. back from the tip, followed by seven ⅛ in. from the tip. This was continued by ⅛-in. increments to the rear of the fin. The seven points in each column were ⅛ in. apart and centered in the submerged portion of the fin surface (see Figure 2).

The soluble fins were inserted in the fin holder, one facing upstream and the other downstream, approximately 18 in. from the leading edge of the holder. This allowed a substantial entrance length, considerably greater than the 4 in. which the work of Boelter et al. (5) indicated as necessary.

Terms Defined

The dissolution measurements, made as described previously, gave the local change in thickness of the benzoic acid. The local mass transport coefficient can be obtained in the following way. A coefficient, k, is defined by the equation

$$N = kA\,(c_s - c) = A\rho\Delta y/\theta \qquad (1)$$

If it is assumed that c_s is much greater than c, then Equation (1) becomes

$$k = \frac{\rho}{c_s}\,\frac{\Delta y}{\theta} \qquad (2)$$

The data are plotted using the Colburn j factor (17) defined as

$$j = \frac{k}{v}\,(N_{Sc})^{2/3} \qquad (3)$$

Flat Plate

In order to determine if the present measurements made in open channel flow could be compared with the results of experiments in other systems, a portion of a 30 in. brass slab was machined away and a 2-in. fin, coated with benzoic acid, was inserted in the slot. This system made it possible to check the results with other studies, both theoretical and experimental, of flow past a flat plate. Local dissolution rates were determined along the surface in the direction of flow. Figure 3 shows these local dissolution rates, expressed as local j factors, plotted vs. the local Reynolds number defined as

$$N_{Re_x} = \frac{xv}{\nu} \qquad (4)$$

Seven measurements at seven different liquid levels for the same value of x are shown at each value of N_{Re_x}.

The theoretical expression for calculating local j factors is based upon the analogy between heat, mass, and momentum transfer. The Blasius solution for the local drag coefficient on a flat plate is

$$f/2 = 0.332\,(N_{Re_x})^{-1/2} \qquad (5)$$

The previously mentioned free-channel laminar streak lines of potassium permanganate and the relatively small local Reynolds numbers (normally transition to turbulence occurs at Reynolds numbers ten to one hundred times greater) justify the use of the Blasius solution in this result.

$f/2$ should be equal to the local j factor in both mass and momentum transfer begin at the leading edge of the slab. However the benzoic acid insert was placed in the brass holder 18¾ in. from the leading edge of the holder. In order to account for this nonsoluble entrance length the correction recommended by Knudsen and Katz (18) for an unheated starting length was used to modify the calculated values of the j factor. This correction is

$$\left[1 - \left(\frac{x_o}{x}\right)^{3/4}\right]^{-1/3} \qquad (6)$$

The value of x_o was 18¾ in. The value of $f/2$ multiplied by the correction term represents the theoretical value of the local j factor. The line on Figure 3 is a plot of this expression.

The data for flat plates can be seen to give reasonable agreement with the theoretical values. The presence of a channel wall across from the soluble test section and the fact that the results are based upon an average velocity and not a free stream velocity appear to be reasonable explanations for the deviation which does occur.

Finned Surfaces

The results of the studies on the dissolution of benzoic acid from the surfaces of transverse fins are presented as

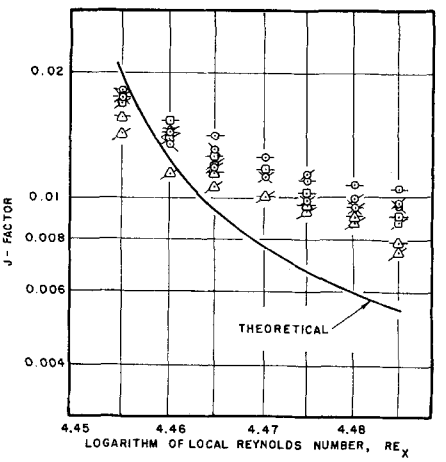

Fig. 3. Local mass transfer coefficients on a flat plate. Mean velocity 0.175 ft/sec. ○ ⅛ in. from bottom, ◇ ¼ in. from bottom, ○ ⅜ in. from bottom, □ ½ in. from bottom, ◇ ⅝ in. from bottom △ ¾ in. from bottom, △ ⅞ in. from bottom.

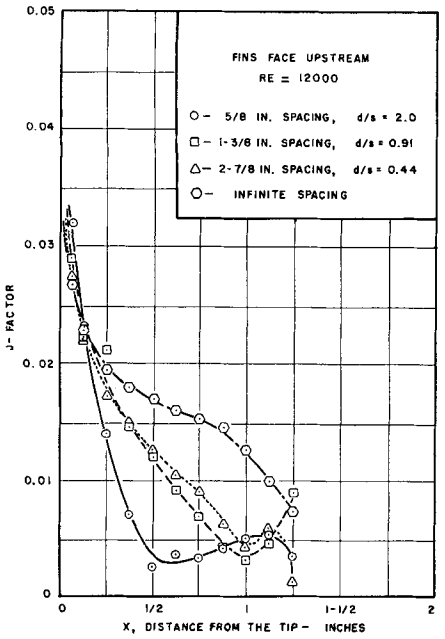

Fig. 4. Effect of fin spacing (fin height is 1¼ in.).

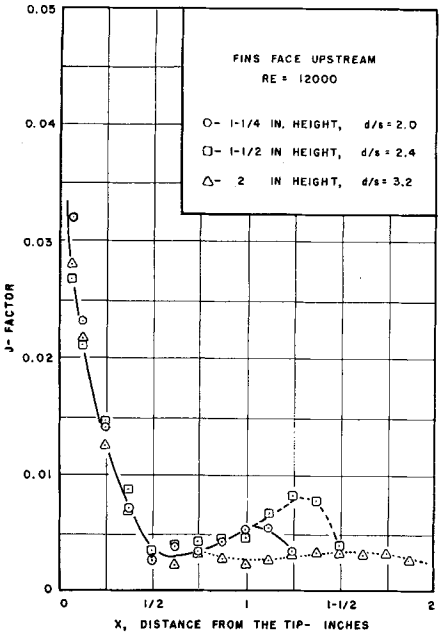

Fig. 6. Effect of fin height (fin spacing is ⅝ in.).

local values of the Colburn j factor vs. the distance, x, measured from the tip of the fin in the direction of the fin root. Each data point is the arithmetic average of the seven measurements made at each value of x (see Figure 2). Figures 4 and 5 show the effect of varying the fin spacing. Figure 4 is for an upstream facing surface.* Figure 5 shows a downstream facing surface. Each figure presents data for the four spacings: ⅝ in., 1⅜ in., 2⅞ in., and infinity.

With reference to Figure 4 it can be seen that the mass transfer rate on an upstream facing surface is a maximum and very large at the tip. If d/s is greater than 1, the rate falls rapidly to a minimum at a point where x is slightly less than s, the fin spacing. If d/s is less than 1, the minimum occurs just before the root at a value of x slightly less than d. It is clear on Figure 4 that the integrated mean value of the transport coefficient increases with fin spacing to a maximum for infinite spacing.

With reference to Figure 5 there is a large value at the tip, but the minimum is reached within a short distance from the tip (this distance ranges from ⅛ to ⅜ in.). A maximum is achieved at a value of x approximately equal to s for d/s greater than 1.

* Note that throughout this paper the fin surface facing upstream is designated the *upstream face* and the surface facing downstream is designated the *downstream face*, see Figure 1.

For d/s less than about 0.7 the j factor does not have a sharp maximum, and for infinite spacing the mean value has diminished considerably. Some evidence of the presence of secondary vortices at the base of the upstream surface is indicated by the rise in the value of the j factor near the fin base as seen in Figure 4.

Figures 6 and 7 show the effect of fin height at constant fin spacing. The results show little variation in the curves over the range of fin heights studied (1¼ to 2 in.). For wider spacings, d/s greater than 0.7, a small decrease in local j factors occurs with an increase of height.

Figures 8 and 9 show the effect of channel width at constant Reynolds number. It is seen that the shape of the curves is the same. There is an increase in j factor with increase in channel width. This increase in j factor actually represents a decrease in the local mass transfer coefficient; the effect of an increase in the velocity term in the j factor expression is greater than the increase in the local coefficient. For the downstream facing fins the maximum j factor near the fin base increases with decreasing channel width.

Figures 10 and 11 show the effect of Reynolds number (changes in velocity at constant channel width) on the local j factor. The upstream surfaces, Figure 10, show a regular decrease in j factor with Reynolds number. For

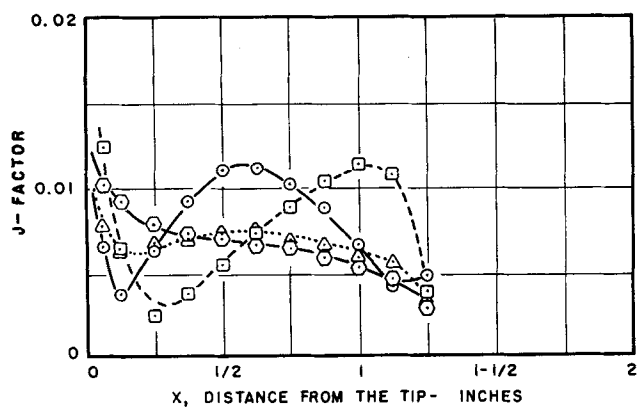

Fig. 5. Effect of fin spacing (fin height is 1¼ in.). Fins face downstream, Re = 12,000. ○ ⅝-in. spacing, d/s = 2.0; □ 1⅜-in. spacing, d/s = 0.91; △ 2⅞-in. spacing, d/s = 0.44; ⬡ infinite spacing.

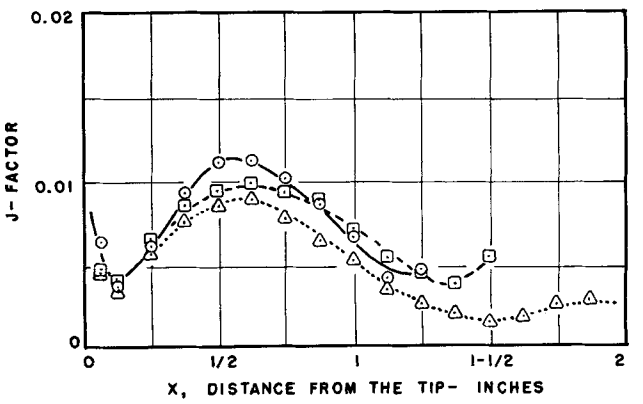

Fig. 7. Effect of fin height (fin spacing is ⅝ in.). Fins face downstream, Re = 12,000. ○ 1¼-in. height, d/s = 2.0; □ 1½-in. height, d/s, = 2.4; △ 2-in. height, d/s = 3.2.

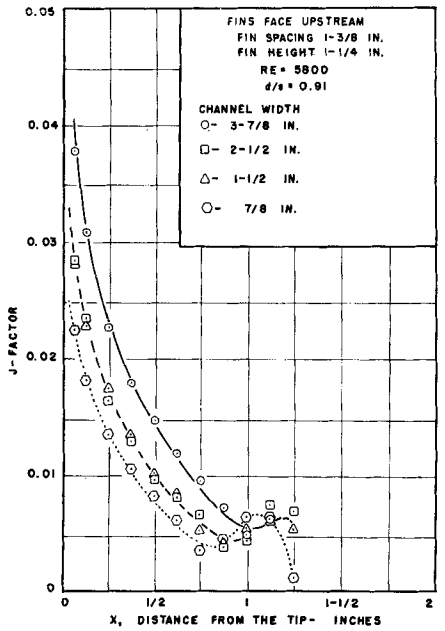

Fig. 8. Effect of channel width.

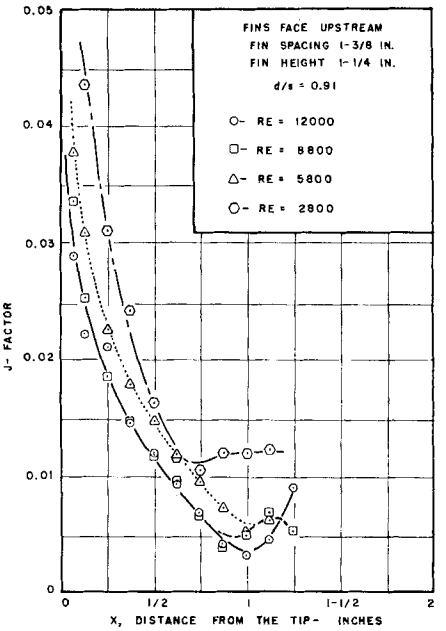

Fig. 10. Effect of Reynolds number.

downstream facing surfaces the curve for $N_{Re} = 2{,}800$ deviates considerably from the trend shown for the other values of N_{Re}. As in the results for the effect of channel width the decrease in j is due to an increased velocity. The value of the mass transfer coefficient increases with increasing Reynolds number.

MEAN RESIDENCE TIMES

The work of Hyman and Corson (*19*) presents an expression for calculating mean residence time from data on the rate of change of solute concentration which is initially at a steady state value and then decreases to zero. The expression for the mean residence time is

$$\theta_m = \int_0^\infty [c(\theta)/c(0)]\, d\theta \qquad (7)$$

The solute used for these measurements was xylene cyanole which forms an opaque blue solution in water. Concentration of the solute in a fin space was measured with a photo resistor which responded to decreases in dye concentration by decreasing in electrical resistance. The circuitry and calculations used in determining mean residence times have been described in detail by Stynes (*20*).

The presence of a boundary layer along the glass bottom of the table causes a velocity gradient in the third dimension, that is in the direction perpendicular to the table surface. These gradients are avoided in determining local mass transfer coefficients by making measurements no closer than ⅛ in. from the surface of the table and no closer than 3/16 in. from the air-water interface. For mean residence times however it is not possible to restrict the xylene cyanole to any specified region of the fin space. As a result of the retention of solute in the low velocity region near the table surface the calculated residence times are probably somewhat higher than would occur in a uniform velocity field. It was assumed that residence time measurements were nevertheless sufficiently reliable to provide a basis for estimating the significance of the rate of interchange of fluid between the main stream and the fin space.

Table 1 presents the calculated values of mean residence times for several geometrical variations. It can be seen from the first six sets of values that fin spacing and height do not affect the residence time of the fluid in the fin space. Significant changes do occur however with variation in the channel width, as shown in the readings near the bottom of the table. This change in channel width occurs at approximately constant velocity and with a decrease in Reynolds number that is proportional to the change in channel width.

Figures 4 to 7 show that the values of the local mass transfer coefficients are strongly dependent upon the fin geometry. Thus it is concluded that the major resistance

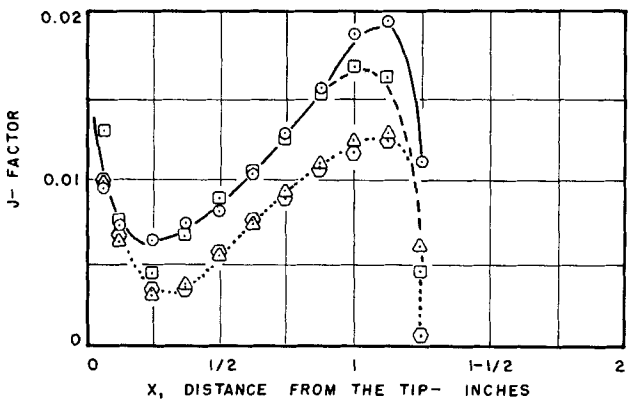

Fig. 9. Effect of channel width. Fins face downstream. Fin spacing 1⅜ in. Fin height 1¼ in. Re = 5,800, d/s = 0.91. ○ 3⅞-in. channel width, □ 2½-in. channel width, △ 1½-in channel width, ○ ⅞-in. channel width.

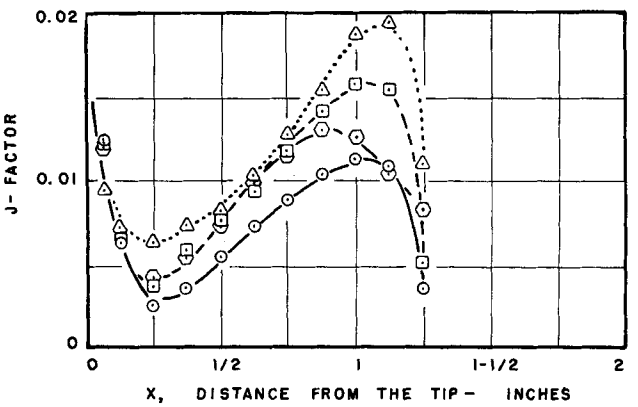

Fig. 11. Effect of Reynolds number. Fins face downstream. Fin spacing 1⅜ in. Fin height 1¼ in. d/s = 0.91. ○ Re = 12,000, □ Re = 8,800, △ Re = 5,800. ○ Re = 2,800.

to transport from finned surfaces is molecular diffusion in the viscous sublayer along these surfaces and not mixing between the main stream and the fluid in the fin space.

VISUAL STUDIES

Visual studies were made over the same range of variables with slow-motion photography. Two different materials were used as tracers in the flowing stream to permit visualization of flow patterns and measurement of fin-space velocities. One of the tracers was xylene cyanole. This dye outlines general flow patterns. The second material was unity oil. It has a specific gravity of one and is immiscible in water. The unity oil was injected at constant pressure into the stream with a 20-gauge hypodermic needle. This method of adding unity oil resulted in the formation of many small spheres, the paths of which traced the flow patterns in the fin space. The motion of the spheres against a background provided by the graph paper on the under side of the table was followed by slow-motion photography (approximately 60 frames/sec.). The relative velocities within the fin space were determined by projecting the movies frame by frame on a screen and measuring the distance traversed by individual spheres for a given number of frames.

The movies (*20*) show the formation of stable vortexes having a diameter approximately equal to the fin spacing with a center displaced slightly downstream from the center of the fin space for d/s equal to or greater than 1. For small values of d/s a vortex of diameter approximately equal to the fin height forms at the upstream face. The formation of small secondary vortexes at the base of the upstream surface was noted in a number of cases. The motion near the tip of the downstream face was seen to be parallel to that face. The spheres here begin to accelerate at a point about ¼ in. from the tip.

Relative velocity measurements show the fin-space velocities to be considerably less than in the main stream. Figures 12*a* and 12*b* show the distance traveled by spheres of unity oil for approximately 0.3 sec. as taken from a typical sequence of fifteen consecutive frames of the movie. It is to be noted in Figure 12*a* that the center of the vortex is not at the center of the fin space but is displaced downstream. The magnitude of the velocities along the upstream face (approximately 30% of the mean velocity of the main stream) is seen to be greater than those along the downstream face (approximately 15% of the mean main stream rate). This difference is even greater where the height-to-spacing ratio is about 0.4, as in Figure 12*b*. Note also that the flow is toward the fin base along the downstream face for d/s equal to 0.4 (Figure 12*b*), whereas the flow is toward the main stream for d/s equal to 0.9 (Figure 12*a*).

FLOW MECHANISM IN THE FIN SPACE

The variation in local mass transfer coefficients along the fin surface and the results of the visual studies which have been presented provide a basis for characterizing the local flow mechanism in the fin space. Fluid from the main stream enters the fin space near the upstream facing surface where the change in direction (to a direction parallel to the fin surface) causes a large transport coefficient. The transport coefficient decreases to a minimum where the vortex is parallel to the fin surface or fin base. In addition to the maximum coefficient at the tip of the upstream-facing surface a maximum occurs at a distance approximately s from the tip of the downstream surface.

Table 1. Mean Residence Times

Fin height, in.	Fin spacing, in.	Channel width, in.	Mean velocity, in./hr.	Residence times, sec.
1½	1¼	3-31/32	17,700	12
1½	1⅜	4-1/16	16,450	11.5
1½	2⅞	4-1/32	17,100	12
1¼	⅝	4-1/32	16,500	11.6
1¼	1¼	3-31/32	16,400	12.8
1¼	1⅜	4	16,400	11.6
1½	1¼	2-31/64	19,800	8.2
1½	1⅜	2½	20,100	8.5
1½	1¼	1	20,100	2.3
1½	1⅜	1	19,700	2.4

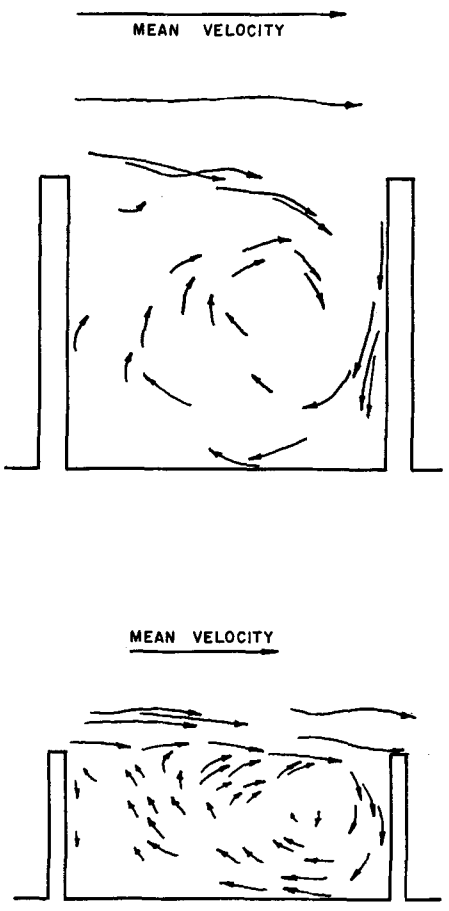

Fig. 12. Flow patterns in the fin space. (Top) *a*. d/s = 0.9. (Bottom) *b*. d/s = 0.4.

For d/s ratios representing a narrow spacing with respect to the height of the fin the primary vortex (with diameter s) is unable to affect the lower portion of the fin space directly. As a result low pressure and transport coefficients generally occur in this lower region. There is some evidence in the literature [see Knudsen and Katz (*4*)] that at high values of the Reynolds number a second vortex of diameter s may form in the base portion of the fin space (d/s would need to be 2 or greater), and this should result in some increase in the coefficients in this region.

For d/s ratios representing relatively wide spacings the primary vortex (of diameter d) does not act directly upon the upstream face. The flow will be away from the main stream along the upstream face (see Figure 12*b*), and the local transport coefficients along this surface will be low. This results in relatively high values of local pressure on the downstream facing surfaces and much lower values along the upstream face. Thus significant form drag occurs owing to the difference in forces acting on opposite surfaces of a fin. This analysis agrees well with the data of Savage and Myers (*10*) who measured large increases in the values of form drag for d/s ratios less than about 0.7.

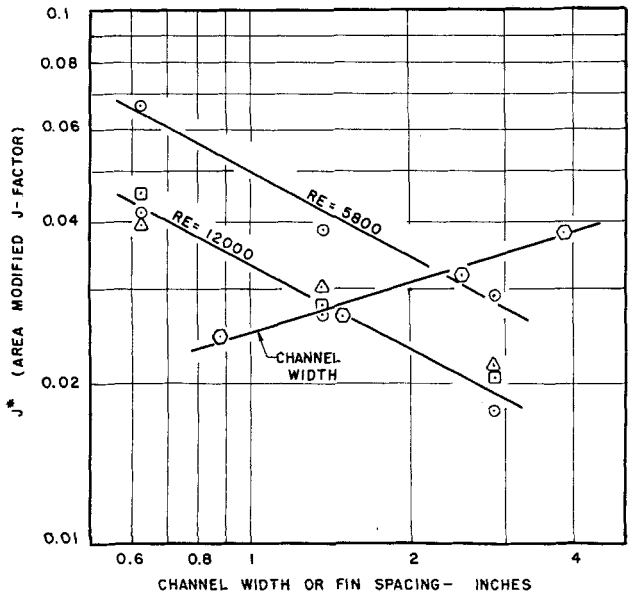

Fig. 13. Effect of channel width and fin spacing.

MEAN VALUES OF THE LOCAL COEFFICIENTS

Integrated mean values of the local coefficients are presented in Table 2. It can be seen from these values that for d/s greater than 1, the upstream and downstream surfaces contribute almost equally to the total transfer from a fin. However more than one third of the total transfer occurs in the distance s from the tip of the upstream face and an equal amount in a distance s centered on the downstream surface. By comparison for fin spaces with d/s less than 0.7 about 65% of the total transport occurs from the upstream face and only 35% from the downstream surface.

There appears to be little or no effect of fin height on the product k_mA_f. Thus it appears that the overall rate of transport depends on the fin spacing but not on the fin height. The fin height may be eliminated as a variable if a new mean mass transfer coefficient k^* is defined in the following way:

$$k^* = \frac{k_mA_f}{A_s} \tag{8}$$

Because the product k_mA_f is independent of fin height the quantity k^* has the same property. The value of A_f/A_s for the experimental system used is found by

$$\frac{A_f}{A_s} = A_c = \frac{2d}{s} + 1 \tag{9}$$

Values of j^* defined as

$$j^* = \frac{k^*}{v}(N_{Sc})^{2/3} \tag{10}$$

are plotted on log-log coordinates in Figure 13 vs. fin spacing for three values of spacing and three of fin height at a Reynolds number of 12,000 and for three spacings (all at the same height) at a Reynolds number of 5,800. The slopes of the two lines are parallel and are equal to −0.53. Figure 13 shows that j^* decreases with increasing fin space when channel width and Reynolds number are maintained constant.

The variation of j^* with channel width D_e is also shown on log-log coordinates in Figure 13. The slope of this line is 0.31. The data are all for a Reynolds number of 12,000, a fin spacing of 1⅜ in., and a fin height of 1¼ in. This increase in j^* is due to the decrease in velocity which occurs and not to an increase in k^* which actually decreases. The exponent 0.31 is low, and it is concluded that the effect of variations in channel width may not be very significant in evaluating mass or heat-transfer rates from finned surfaces. (Channel width will of course be of great importance in determinating power requirements.) Boelter et al. (5) found no effect of channel width in their heat transfer study.

Figure 14 shows the effect of Reynolds number on j^*. The data are for a 1¼ in. height, 1⅞-in. channel width, and three different fin spacings. The lines are essentially parallel, and their slope is −0.65. The exponent 0.65 for the effect of Reynolds number was also obtained by Boelter et al. (5) and Brouillette et al. (7).

As it is usually expressed j depends only upon the Reynolds number. The addition of fins to the surface makes it necessary to consider additional terms in order to account for the difficulty in describing geometrically similar conditions under these circumstances. It can be seen from Figures 13 and 14 that log j^* varies linearly with the logs of fin spacing, channel width, and Reynolds number. Assuming these to be the significant variables in defining j^* then one may write

$$j^* = R_1\left[\frac{D_e^{0.31}}{N_{Re}^{0.65}\,(s)^{0.53}}\right] + R_2 \tag{11}$$

Table 2. Summary of Calculated Mean Values

s, in.	d, in.	D_e, in.	N_{Re}	$(K_m)_U$, in./hr.	$(K_m)_D$, in./hr.	$(K_m)_O$, in./hr.	j^*
∞	1¼	3⅞	12,000	2.65	1.20	1.93	0.0068
1⅜	1¼	3⅞	12,000	1.79	1.30	1.55	0.0270
⅝	1¼	3⅞	12,000	1.39	1.23	1.31	0.0418
2⅞	1¼	3⅞	12,000	1.91	1.04	1.48	0.0177
⅝	1½	3⅞	12,000	1.36	1.07	1.22	0.0455
1⅜	1½	3⅞	12,000	1.58	1.10	1.34	0.0278
2⅞	1½	3⅞	12,000	1.86	1.25	1.56	0.0203
⅝	2	3⅞	12,000	0.92	0.75	0.84	0.0398
1⅜	2	3⅞	12,000	1.47	0.98	1.23	0.0307
2⅞	2	3⅞	12,000	1.51	1.35	1.43	0.0219
⅝	1¼	3⅞	5,800	1.07	0.95	1.01	0.0665
1⅜	1¼	3⅞	5,800	1.16	0.92	1.04	0.0386
2⅞	1¼	3⅞	5,800	1.34	0.97	1.16	0.0291
1⅜	1¼	3⅞	8,800	1.45	1.19	1.32	0.0326
1⅜	1¼	2½	5,800	1.33	1.32	1.33	0.0323
1⅜	1¼	1½	5,800	2.27	1.67	1.97	0.0279
1⅜	1¼	⅞	5,800	3.13	2.74	2.94	0.0246

$(K_m)_U$, $(K_m)_D$, and $(K_m)_O$ are the values of the mean mass-transfer coefficient on the upstream surface, the downstream surface, and overall, respectively.

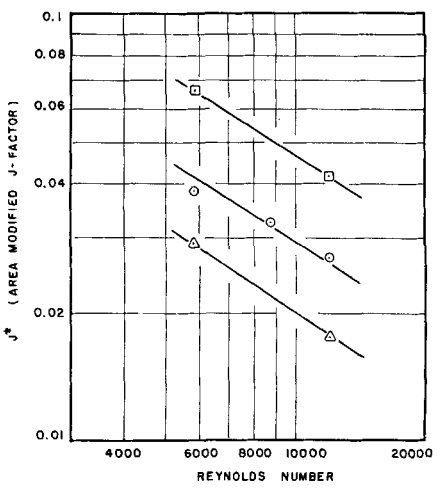

Fig. 14. Effect of Reynolds number. Fin height 1¼ in. ○ 1⅜-in. spacing, □ ⅝-in. spacing, △ 2⅞-in. spacing.

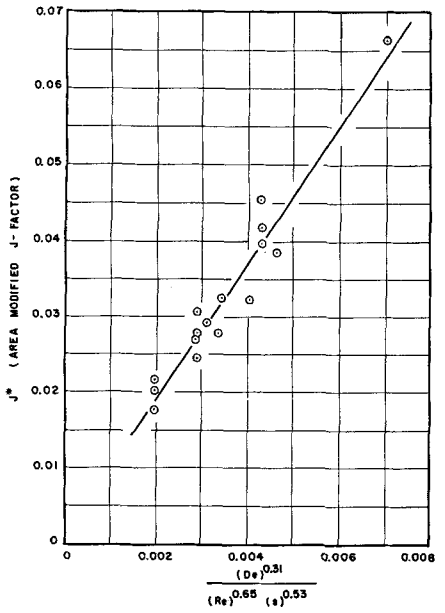

Fig. 15. Mass transfer correlation.

where R_1 and R_2 are constants which may be determined by plotting j^* vs. the quantity in parenthesis. This has been done in Figure 15. The resulting expression as determined by the method of least squares is

$$j^* = 9.0\left[\frac{(D_e)^{0.31}}{(N_{Re})^{0.65}\,(s)^{0.53}}\right] + 0.0012 \qquad (12)$$

The mean deviation from the line is 7%, while the maximum deviation is 16.5%. The standard deviation is 0.0028.

TUBES WITH EXTERNAL OR INTERNAL FINS

Extension of the form of Equation (11) to tubes with external or internal fins depends upon defining a proper value for the area coefficient A_c in k^*. The value determined for A_c in Equation (9) is for a fin for which the surface area for a given increment of height is constant with distance from the tip. This is not true for internal or external transverse fins on a tube wall for which the area increases or decreases, respectively, with distance from the fin tip.

External fins increase in area available for transport as the fin height is increased (for a given tube diameter). This favors larger transport rates for taller fins, since the region of highest local coefficients (as found in this study) is being supplied with additional area for transfer. Thus it is to be expected that the product k_mA_f might not be independent of fin height.

Internal fins provide exactly the opposite problem. Here the area is a maximum where the local coefficients are low, and lower rates of transport may be expected in general for internal fins as compared with external fins containing the same total area and base temperature. The data of Savage and Myers (*10*), which is for relatively tall internal fins at small d/D_e values, can be correlated by Equation (1). It was assumed that

$$A_c = \left[\frac{d}{2s} + 1\right]\frac{D}{D_e} \qquad (13)$$

in which D is the tube diameter. This takes only one half of the total surface area of the fin into account. This resulted in the following expression for j^*:

$$j^* = 4.17\left[\frac{(D_e)^{0.31}}{(N_{Re})^{0.65}\,(s)^{0.53}}\right] + 0.00603 \qquad (14)$$

j^* for heat transfer is defined as

$$j^* = \frac{h_mA_c}{C_pG}(N_{Pr})^{2/3} \qquad (15)$$

The mean deviation from the equation is 5%, and the maximum deviation is 18.3%. The standard deviation is 0.00066. This good agreement is attributed to the fact that the data are for a 6-in. tube with fins about 1 in. in height which to a certain extent simulates the geometry of the present study.

OPTIMUM SPACING

In order to determine the optimum fin spacing it is necessary to specify the conditions which are to be optimized. In this study it was desirable to know what fin spacing would give the maximum mass transfer rate per unit of concentration gradient. Thus it was necessary to maximize the product k_mA_t. From Equations (8), (9), and (10)

$$j^* = \frac{k_m}{v}(N_{Sc})^{2/3}\left(\frac{2d}{s} + 1\right) \qquad (16)$$

From Equation (11) j^* is also defined as

$$j^* = \left[\frac{R_1\,(D_e)^{0.31}}{(N_{Re})^{0.65}\,(s)^{0.53}}\right] + R_2 \qquad (17)$$

These are combined and written in terms of k_mA_t as

$$k_mA_t = \left[\frac{R_1\,(D_e)^{0.31}\,v\,s}{(N_{Re})^{0.65}\,(s)^{0.53}\,N_{Sc})^{2/3}\,(2d+s)} + \frac{R_2\,v\,s}{(N_{Sc})^{2/3}\,(2d+s)}\right]A_t \qquad (18)$$

The area is given by

$$A_t = (2d + s)\,bL/(s + t) \qquad (19)$$

It is to be noted that this neglects the area of the fin tip. Let

$$\beta = \frac{R_1\,(D_e)^{0.31}}{R_2\,(N_{Re})^{0.65}} \qquad (20)$$

Let

$$\psi = \frac{R_2\,v\,L\,b}{(N_{Sc})^{2/3}} \qquad (21)$$

Then

$$k_mA_t = \left[\frac{\beta\,s}{(s)^{0.53}\,(s+t)} + \frac{s}{s+t}\right]\psi \qquad (22)$$

When one takes the derivative with respective to s (assuming β and ψ are independent of s) a maximum exists if

$$\frac{1}{(s)^{0.53}}(s - 0.887\,t) = \frac{t}{0.53\,\beta} \qquad (23)$$

It can be shown from Equation (23) that the optimum value of fin spacing is approximately equal to the fin thickness even for Reynolds numbers over 100,000. A similar analysis applies to the heat transfer data correlation developed for the data of Savage and Myers (*10*). It is to be noted however that neither the data of this study nor that of Savage and Myers were for fin spacings as small as the fin thickness.

Comparison of this predicted optimum with the data of Knudsen and Katz (*4*), Sams (*6*), and Brouillette et al. (*7*) shows that in each case the experimental finned tube giving the maximum value of the product h_mA_t is the one with a spacing most nearly equal to the fin thickness. These studies do use fin spacings nearly as small as the fin thickness. This provides good support for the optimums predicted on the basis of the much wider spacings used in this study. Since spacings which approximate the fin thickness are quite small in general, it can be concluded that

the large increase in area resulting for many fins per inch is more important in increasing the heat transfer rate than is the increased value of the transport coefficient which would be obtained if wider spacings were used.

SUMMARY

Data have been presented showing the variation in the local Colburn j factor as a function of fin spacing, fin height, channel width, and Reynolds number. Mean values of the local j factors are correlated as an area-modified j factor vs. fin spacing, channel width, and Reynolds number. Measurements of local dissolution rates, made on flat plates at several velocities, give reasonable agreement with theoretical values based upon the analogy between heat, mass, and momentum transfer.

Visual studies combined with the above data for local coefficients give a picture of the flow mechanism within the fin space. This is dominated by a primary vortex with a diameter which depends upon the ratio of fin height to fin spacing. Three regions with distinctly different flow character are defined for d/s less than 0.7, d/s between 0.7 and 1.5, and d/s greater than 1.5. The results give good agreement with the data of Harris and Wilson (*11*) for local heat transfer coefficients and with those of Tani et al. (8), Roshko (9), and Savage and Myers (*10*) for local pressure measurements.

Mean residence times of the fluid in the fin space have been investigated and shown to be independent of the fin height and fin spacing. This leads to the conclusion that the controlling resistance to transport from finned surfaces is the rate of molecular diffusion through the viscous sublayer along the fin surface and not the rate of mixing between the main stream and the fin space.

The design of a transport system using rectangular fins with flow normal to the fin surface depends upon whether the fins are internal or external to a tube or attached to a flat plate as in the present study. In each of these cases the optimum fin spacing appears to be one which is approximately equal to the fin thickness. This conclusion is supported by the work of Knudsen and Katz (*4*), Sams (*6*), and Brouillette et al. (*7*). The data of Savage and Myers (*10*) show that d/s should be 1 or greater to avoid high drag coefficients. For internal fins a height equal to the spacing would appear to be optimum as increasing the height beyond this value decreases the area available for heat transfer in the region of maximum local coefficient (that is the tip). For external fins however increasing the height to obtain large d/s values would appear to increase the net heat transfer potential, as the area increases at the tip in this case.

The effect of increasing Reynolds number and decreasing channel width is to increase the transport coefficients. This also increases the velocity in the channel, and since the total friction occuring in a channel is a power function of the velocity, great care must be taken when varying these parameters to obtain higher heat transfer coefficients.

NOTATION

A = elemental area (sq. in.)
A_c = area correction equal to A_f/A_s
A_f = total surface area in fin space (sq. in.)
A_s = area common to fin space and free channel (sq. in.)
A_t = area A_f times number of fin spaces in length L (sq. in.)
b = depth of liquid above table surface (in.)
c = mixing-cup concentration of benzoic acid (g./liter)
c_s = solubility of benzoic acid in water (g./liter)
C_p = specific heat of water (B.t.u./lb-°F.)
d = fin height (in.)
D = inside diameter (in.)
D_e = equivalent diameter as defined in Figure 1 (in.)
f = drag coefficient defined by Equation (7)
G = mass velocity (lb./hr.-sq. ft.)
h_m = mean heat transfer coefficient (B.t.u./hr.-sq. ft.-°F.)
j = local j factor defined by Equation (5)
j^* = modified j factor defined by Equation (16)
k = local mass transfer coefficient (in./hr.)
k_m = mean mass transfer coefficient (in./hr.)
k^* = modified mean mass transfer coefficient (in./hr.)
N = mass transfer rate (g./hr.)
N_{Pr} = Prandtl number
R = constants
N_{Re} = Reynolds number based upon D_e and v
N_{Rex} = Reynolds number defined by Equation (6)
s = fin spacing (in.)
N_{Sc} = Schmidt number
t = fin thickness (in.)
v = bulk velocity defined as $V/b\ D_e$ (in./hr.)
V = volumetric flow rate (cu. in./hr.)
x = distance from leading edge of soluble surface (in.)
x_o = distance from leading edge of flat plate (in.)
Δy = thickness of benzoic acid removed (in.)

Greek Letters

β = defined by Equation (27)
θ = time (hr.)
θ_m = mean residence time (sec.)
μ = viscosity (centipoise)
ν = kinematic viscosity (in./hr.)
ρ = density (lb./cu. ft.)
ψ = defined by Equation (28)

LITERATURE CITED

1. Jakob, M., "Heat Transfer," Vol. 1, p. 217, Wiley, New York (1958).
2. Avrami, M., and J. B. Little, *J. App. Phys.*, **13**, 255 (1942).
3. Gardner, K. A., *Trans. Am. Soc. Mech. Engrs.*, **67**, 621 (1945).
4. Knudsen, J. G., and D. L. Katz, *Chem. Eng. Progr.*, **46**, 490 (1950).
5. Boelter, L. M. K., G. Young, M. L. Greenfield, V. D. Sanders, and M. Morgan, *Natl. Advisory Comm. Aeronaut. Tech. Note 2517* (1951).
6. Sams, E. W., *Natl. Advisory Comm. Aeronaut. Research Memorandum E52D17* (1952).
7. Brouillette, E. C., T. R. Mifflin, and J. E. Myers, *Am. Soc. Mech. Engrs. Paper No. 57-A-47* (1957).
8. Tani, I., M. Iuchi, and H. Komoda, *Aeronaut. Research Instit., U. of Tokyo Rept. 364*, **27**, 119 (1961).
9. Roshko, A., *Natl. Advisory Comm. Aeronaut. Tech. Note 3488* (1955).
10. Savage, D. W., and J. E. Myers, *A.I.Ch.E. Journal*, **9**, 694 (1963).
11. Harris, M. J., and J. T. Wilson, *J. Brit. Nucl. Energy Conf.* **6**, 330 (1961).
12. Sherwood, T. K., *Ind. Eng. Chem.*, **42**, 2077 (1950).
13. King, C. V., and S. S. Brodie, *J. Am. Chem. Soc.*, **59**, 1375 (1937).
14. Garner, F. H., and R. D. Suckling, *A.I.Ch.E. Journal*, **4**, 114 (1958).
15. Linton, W. H., and T. K. Sherwood, *Chem. Eng. Progr.*, **46**, 258 (1950).
16. Danckwerts, P. V., and C. Anolick, *Trans. Inst. Chem. Engrs.*, **40**, 203 (1962).
17. Colburn, A. P., *Trans. Am. Inst. Chem. Engrs.*, **29**, 174 (1933).
18. Knudsen, J. G., and D. L. Katz, "Fluid Dynamics and Heat Transfer," p. 260, McGraw-Hill, New York (1958).
19. Hyman, D., and W. B. Corson, *Ind. Eng. Chem., Process Design Devlop.*, **1**, 92 (1962).
20. Stynes, S. K., Ph.D. thesis, Purdue University, Lafayette, Indiana (1963).

Manuscript received June 12, 1963; revision received December 18, 1963; paper accepted December 19, 1963.